Linear response theory for electron-hole pair kinetics: Exciton formation

Shota Ono*

Department of Physics, Graduate School of Engineering,Yokohama National University, Yokohama 240-8501, Japan
and Department of Physics, University of California, Berkeley, California 94720-7300, USA

(Received 30 April 2015; published 1 September 2015)

A linear response theory for electron-hole pair density is developed, which constitutes a theoretical method, and a definition of exciton density in a first-principles context is derived by considering both the electron-hole attractive interaction and the screening effect. This allows the exciton time evolution to be examined. This formulation is applied to a jellium model in order to prove the existence of a transient exciton, and to observe crossover from a transient to a stable exciton in response to decreased electron density. The exciton formation mechanism is also revealed.

DOI: 10.1103/PhysRevB.92.125101 PACS number(s): 71.10.−w, 71.35.−y, 78.47.da

I. INTRODUCTION

The exciton is one of the most important elementary excitations in condensed matter. Intense peaks below the single-particle absorption edge of the optical absorption spectra of molecules, semiconductors, and insulators indicate the presence of these particles [1,2]. This is particularly true for systems with high dielectric constants, in which the effective-mass approximation may be valid [3].

It is believed that exciton observation in metals is quite difficult, because free carriers immediately screen the holes created by photon absorption. Recently, however, Cui *et al.* have reported that excitons exist in metals in the form of *transient* excitons, based on findings obtained through the application of multiphoton photoemission spectroscopy to a silver surface [4]. The transient excitonic state that does not correspond to anything in the single-particle band structure develops into an image potential state within 100 fs, which is quite short compared to the exciton lifetime in typical insulators. The findings of this experiment pose the question of how to define the existence of an exciton within a short time scale, and move the field in the direction of developing an understanding of excitons in both space and time.

The screening effect is significant as regards exciton existence. After the creation of the photohole, the Coulomb potential between the electrons and holes is gradually weakened over time [5]. Since screening is incomplete in an insulator, the Coulomb potential approaches an approximate ratio of the bare Coulomb potential and the dielectric constant, which causes long-lived excitons to appear. On the other hand, the screening in a metal is complete. The Coulomb potential approaches the well-known Tomas-Fermi potential, which generates no bound states in general [6]. However, Schöne and Ekardt have theoretically suggested the possibility of transient excitons occurring in bulk metals until screening completion, although this is a very short time scale [7,8]. A similar conclusion has been reached by Gumhalter *et al.*, via a systematic calculation for metal surfaces [9]. In both studies, the transient excitons are described by an effective-mass equation under a time-dependent potential for the electron, which is calculated using a linear response theory. In this approach, two bands relevant to the exciton formation must be chosen *a priori*, which may introduce an arbitrariness to the definition. The Bethe-Salpeter equation (BSE) is, in principle, an exact scheme describing the excitonic properties of electronic systems beyond the effective-mass approximation [10]. However, the present method of solving the BSE can be applied to a system under a stationary interaction potential only. Thus, to understand the kinetics of the exciton, it is highly desirable to develop a theory that passes beyond both the effective-mass approximation and the use of a stationary interaction potential in the BSE. Note that, although Attaccalite *et al.* have derived an equation of motion for the nonequilibrium Green's function that may be regarded as a time-dependent BSE [11], the application of this theory has been limited to the calculation of the optical absorption spectra in finite systems and wide-gap semiconductors.

In this paper, a theory that allows the kinetics of the exciton to be described is developed. This approach is based on a linear response theory for the electron-hole (EH) pair density, which allows direct computation of the time-dependent EH pair density fluctuations under an external perturbation. A natural definition of the exciton is derived by considering the EH attractive interaction and the screening effect. Application to a jellium model proves the existence of the transient exciton and reveals a property of the time evolution of exciton formation.

II. FORMULATION

We consider an EH pair density operator defined as

$$n_2(x,x') = \psi^\dagger(x')\psi(x)\psi^\dagger(x)\psi(x'), \tag{1}$$

where x and x' represent the position ($\boldsymbol{x}$ and $\boldsymbol{x}'$) and spin (σ and σ') of the electron and hole, respectively. The expectation value of this operator with respect to the ground state is equivalent to the EH pair density in the system

$$\langle N,0|n_2(x,x')|N,0\rangle = \sum_S |\langle N,S|\psi^\dagger(x)\psi(x')|N,0\rangle|^2, \tag{2}$$

where $|N,S\rangle$ is an arbitrary excited state in the N-electron system. A carefully selected perturbation excites the excitons, and their decay can be studied within the framework of a linear response theory. In general, the interaction Hamiltonian between a system of charged particles and the electromagnetic

*shota-o@ynu.ac.jp

field is the sum of the scalar and vector potential components, such that

$$H'(t) = H'_s(t) + H'_v(t). \tag{3}$$

Then, the linear response is expressed by

$$\delta\langle n_2(x,x';t)\rangle = \frac{i}{\hbar}\int dt'\langle N,0|[H'(t'),n_2(x,x';t)]|N,0\rangle. \tag{4}$$

Here, $\delta\langle n_2(x,x';t)\rangle$ describes the induced EH pair density at time t (an electron and hole at x and x', respectively) caused by an external perturbation at t'. As a simple example, we consider a scalar potential

$$H'(t) = -\int dx e\varphi^{\rm ext}(\boldsymbol{x};t)n_1(x;t), \tag{5}$$

where e is the charge, $\varphi^{\rm ext}(\boldsymbol{x};t)$ is the time-dependent and spin-independent scalar potential, and $n_1(x;t)$ is the electron density operator in the Heisenberg picture, $n_1(x;t) = e^{iHt/\hbar}\psi^\dagger(x)\psi(x)e^{-iHt/\hbar}$ (H is the unperturbed Hamiltonian). If the retarded correlation function is defined by

$$D_2^{\rm R}(x,x',x'';t-t') = -i\theta(t-t')\langle N,0|[n_2(x;x';t),n_1(x'';t')]|N,0\rangle, \tag{6}$$

Eq. (4) may be rewritten as

$$\delta\langle n_2(x;x';t)\rangle = -\frac{e}{\hbar}\int dx''\int_{-\infty}^{\infty}dt' \times\varphi^{\rm ext}(\boldsymbol{x}'';t')D_2^{\rm R}(x,x',x'';t-t'). \tag{7}$$

The computation of $\delta\langle n_2(x,x';t)\rangle$ enables us to derive the lifetimes of the excitons in the system in question under a certain excitation. Here, we consider a homogeneous system whose Hamiltonian is written as (see Ref. [12])

$$H = H_0 + H_1 = \int dx\psi^\dagger(x)\left(-\frac{\hbar^2}{2m}\nabla^2\right)\psi(x) + \frac{1}{2}\int dx\int dx'\psi^\dagger(x)\psi^\dagger(x')V(\boldsymbol{x}-\boldsymbol{x}')\psi(x')\psi(x), \tag{8}$$

where H_0 is the noninteracting Hamiltonian describing the kinetic energy of the electron systems and H_1 is the perturbation Hamiltonian describing the interaction energy between the electrons at position $\boldsymbol{x}$ and $\boldsymbol{x}'$ via $V(\boldsymbol{x}-\boldsymbol{x}')$. In this system, $D_2^{\rm R}(x,x',x'';t-t')$ is a function of $\boldsymbol{x}-\boldsymbol{x}''$ and $\boldsymbol{x}'-\boldsymbol{x}''$, and the Fourier transformation is defined as

$$\tilde{D}_2^{\rm R}(q,q',\sigma'';\omega) = \int d(\boldsymbol{x}-\boldsymbol{x}'')\int d(\boldsymbol{x}'-\boldsymbol{x}'') \times e^{-i\boldsymbol{q}\cdot(\boldsymbol{x}-\boldsymbol{x}'')}e^{-i\boldsymbol{q}'\cdot(\boldsymbol{x}'-\boldsymbol{x}'')}\int d(t-t')e^{i\omega(t-t')} \times D_2^{\rm R}(x,x',x'';t-t'), \tag{9}$$

where $q = (\boldsymbol{q},\sigma)$ denotes the wave vector and spin. The time dependence of the EH pair density in the momentum space is expressed as

$$\delta\langle\tilde{n}_2(q,q';t)\rangle = \sum_{\sigma''}\int\frac{d\omega}{2\pi}e^{-i\omega t}\frac{(-e)}{\hbar}\tilde{\varphi}^{\rm ext}(\boldsymbol{q}+\boldsymbol{q}';\omega) \times\tilde{D}_2^{\rm R}(q,q',\sigma'';\omega). \tag{10}$$

Equation (10) can also be extended to treat the reciprocal-lattice vector, which enables us to study periodic systems. To evaluate $\tilde{D}_2^{\rm R}(q,q',\sigma'';\omega)$, we first consider a time-ordered correlation function:

$$D_2^{\rm T}(x,x',x'';t-t') = -i\langle N,0|{\rm T}[n_2(x,x';t)n_1(x'';t')]|N,0\rangle. \tag{11}$$

The perturbation expansion method can be used, because of the presence of the time-ordering operator T in Eq. (11). The Fourier transformations of the time-ordered correlation function of $D_2^{\rm T}$ for space and time are given as, respectively,

$$\tilde{D}_2^{\rm T}(q,q',\sigma'';\omega) = \int d(\boldsymbol{x}-\boldsymbol{x}'')\int d(\boldsymbol{x}'-\boldsymbol{x}'') \times e^{-i\boldsymbol{q}\cdot(\boldsymbol{x}-\boldsymbol{x}'')}e^{-i\boldsymbol{q}'\cdot(\boldsymbol{x}'-\boldsymbol{x}'')}D_2^{\rm T}(x,x',x'';\omega) \tag{12}$$

and

$$D_2^{\rm T}(x,x',x'';\omega) = \int d(t-t')e^{i\omega(t-t')}D_2^{\rm T}(x,x',x'';t-t'). \tag{13}$$

Using the relations in a frequency (ω) representation $D_2^{\rm T}(x,x',x'';\omega) = D_2^{\rm R}(x,x',x'';\omega)$ for $\omega > 0$ and $D_2^{\rm R}(x,x',x'';-\omega) = D_2^{\rm R*}(x,x',x'';\omega)$, one can obtain $D_2^{\rm R}(x,x',x'';\omega)$ for all values of ω (Ref. [13]). Finally, $\tilde{D}_2^{\rm R}(q,q',\sigma'';\omega)$ can be obtained after Fourier transforming the space dependence, as given by Eq. (12).

III. EXCITON DESCRIPTION

To study the exciton existence, we must consider the competing effect between the electron-hole attractive interaction and the screening, because the former determines the two-particle trend, while the latter gives rise to the single-particle behavior.

We study the attractive interaction using the perturbation expansion of $D_2^{\rm T}(x,x',x'';t-t')$ given by Eq. (11). The evaluation of $D_2^{\rm T}(x,x',x'';\omega)$ is performed by using the noninteracting Green's function:

$$G^{(0)}(x,x';\omega) = \delta_{\sigma\sigma'}G_\sigma^{(0)}(\boldsymbol{x},\boldsymbol{x}';\omega) = \delta_{\sigma\sigma'}\left(\sum_\alpha^{\rm occ}\frac{\phi_{\alpha\sigma}(\boldsymbol{x})\phi^*_{\alpha\sigma}(\boldsymbol{x}')}{\omega-\omega_\alpha-i\delta}+\sum_\beta^{\rm emp}\frac{\phi_{\beta\sigma}(\boldsymbol{x})\phi^*_{\beta\sigma}(\boldsymbol{x}')}{\omega-\omega_\beta+i\delta}\right), \tag{14}$$

where $\phi_{\alpha\sigma}(\boldsymbol{x})$ denotes the single-particle eigenfunction with quantum number α and spin σ for the noninteracting Hamiltonian. The product of ω_α and the Planck constant $\hbar$ is the energy of the single-particle state α. "occ" and "emp" denote

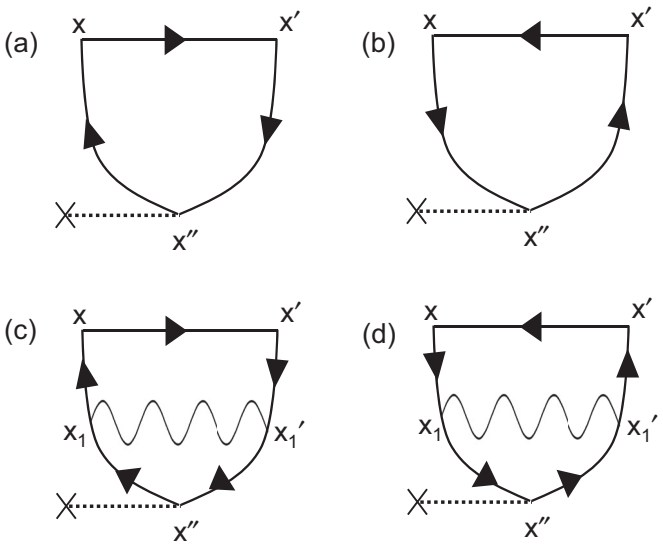

FIG. 1. Contribution to $D_2^{\mathrm{T}}(x,x',x'';t-t')$. (a) and (b) are zeroth order, while (c) and (d) show the first-order contribution. The cross and the dotted line indicate the external perturbation, and the wavy line indicates the Coulomb interaction.

the occupied states α and empty states β, respectively. The fact that the noninteracting Hamiltonian does not change the spin of the electron and hole is assumed. In the homogeneous system described by Eq. (8), the single-particle eigenfunction for H_0 is expressed by the plane waves:

$$\phi_{\alpha\sigma}(\boldsymbol{x}) = \frac{1}{\sqrt{\Omega}} e^{i\boldsymbol{k}_\alpha\cdot\boldsymbol{x}} s(\sigma), \tag{15}$$

where $\boldsymbol{k}_\alpha$ is the wave vector, $s(\sigma)$ is the spin function, and Ω is the volume of the system. Then, the summation in Eq. (14) is replaced by the following integral:

$$\sum_{\alpha}^{\mathrm{occ}} = \int d\boldsymbol{k}_\alpha \frac{\Omega}{(2\pi)^3}\theta_H(k_F - |\boldsymbol{k}_\alpha|), \tag{16}$$

$$\sum_{\beta}^{\mathrm{emp}} = \int d\boldsymbol{k}_\beta \frac{\Omega}{(2\pi)^3}\theta_H(|\boldsymbol{k}_\beta| - k_F), \tag{17}$$

where $\theta_H(k)$ is the Heaviside step function and k_F is the Fermi wave number. Figure 1 shows the Feynman diagram appropriate for describing exciton creation. No attractive interaction is included in the zeroth-order diagrams [Figs. 1(a) and 1(b)], while attractive interaction is included in the first-order diagrams [Figs. 1(c) and 1(d)]; this enhances the EH pair density as a result of the exciton creation. Details of this calculation are given in the Appendix.

Schöne and Ekardt [7] studied the screening effect in a jellium model by computing the linear response of the total potential to the sudden creation of a potential induced by a positive charge, with

$$\varphi^{\mathrm{ext}}(\boldsymbol{x};t) = \frac{e}{|\boldsymbol{x}|}\theta(t), \tag{18}$$

where $\theta(t)$ is a step function. Within an adiabatic approximation, such a potential can create bound states at $t=0$. The total potential for the single-particle state varies dynamically because of the screening effect and is expressed by the sum of the external and induced potentials:

$$\begin{aligned}\tilde{\varphi}^{\mathrm{tot}}(\boldsymbol{q};t) &= \tilde{\varphi}^{\mathrm{ext}}(\boldsymbol{q};t) + \tilde{\varphi}^{\mathrm{ind}}(\boldsymbol{q};t),\\ &= \frac{4\pi e}{|\boldsymbol{q}|^2}\left\{1+\frac{8e^2}{\hbar|\boldsymbol{q}|^2}\int_0^\infty \frac{d\omega}{\omega}\mathrm{Im}\tilde{D}_1^{\mathrm{R}}(\boldsymbol{q};\omega)(1-\cos\omega t)\right\}\theta(t),\end{aligned} \tag{19}$$

where $\tilde{D}_1^{\mathrm{R}}(\boldsymbol{q};\omega)$ is the retarded density-density correlation function [7,12]. Solving the effective-mass equation with the use of Eq. (19) yields bound states with time-dependent energy. For large time values, the total potential approaches the Tomas-Fermi potential, $\sim(q_{\mathrm{TF}}^2+|\boldsymbol{q}|^2)^{-1}$ (q_{TF} is the Tomas-Fermi wave vector), resulting in an absence of bound states. The use of $\tilde{\varphi}^{\mathrm{tot}}(\boldsymbol{q};\omega)$ in Eq. (19) as an external potential together with Eq. (10) enables us to simultaneously study both the attractive interaction effect and the screening effect on the dynamics of the EH pair. We obtain

$$\delta\langle\tilde{n}_2(q,q';t)\rangle = -\frac{2e^2}{\hbar|\boldsymbol{q}+\boldsymbol{q}'|^2}(I_0+I_1)\theta(t), \tag{20}$$

where

$$I_0 = 4\int_0^\infty \frac{d\omega'}{\omega'}\mathrm{Im}\tilde{D}_2^{\mathrm{R}}(q,q',\sigma'';\omega')(1-\cos\omega' t), \tag{21}$$

$$\begin{aligned}I_1 = \frac{8e^2}{\hbar|\boldsymbol{q}+\boldsymbol{q}'|^2}\int_0^\infty \frac{d\omega_0}{\omega_0}\mathrm{Im}\tilde{D}_1^{\mathrm{R}}(\boldsymbol{q}+\boldsymbol{q}';\omega_0)\\ \times\left[I_0 - 4\int_0^\infty \frac{d\omega'}{\omega'}\mathrm{Im}\tilde{D}_2^{\mathrm{R}}(q,q',\sigma'';\omega')C(\omega_0,\omega')\right].\end{aligned} \tag{22}$$

Here, $C(\omega_0,\omega') = \omega'^2(\cos\omega_0 t - \cos\omega' t)/(\omega'^2-\omega_0^2)$, I_0 represents the EH pair creation, and I_1 describes the EH pair annihilation due to the screening. Note that Eq. (20) is regarded as a generalization of the work of Canright [14], in which the transient screening response of the electron gas to a suddenly created point charge, $\delta\langle n_1(x;t)\rangle$, is calculated. Given that the stability of the exciton is determined by the previously mentioned competing effect, we define the exciton density as

$$\tilde{n}_{\mathrm{exc}}(\boldsymbol{q},\boldsymbol{q}';t) = \sum_{\sigma,\sigma'}\tilde{n}_{\mathrm{exc}}(q,q';t), \tag{23}$$

$$\tilde{n}_{\mathrm{exc}}(q,q';t) = \delta\langle\tilde{n}_2(q,q';t)\rangle - \delta\langle\tilde{n}_2^{(0)}(q,q';t)\rangle, \tag{24}$$

where

$$\delta\langle\tilde{n}_2^{(0)}(q,q';t)\rangle = -\frac{2e^2}{\hbar|\boldsymbol{q}+\boldsymbol{q}'|^2}I_0^{(0)}\theta(t), \tag{25}$$

with $I_0^{(0)}$ being the zeroth-order contribution of Eq. (21). Both the attractive interaction between the electron and hole and the screening effect are included in $\delta\langle\tilde{n}_2(q,q';t)\rangle$, while no such effects are included in $\delta\langle\tilde{n}_2^{(0)}(q,q';t)\rangle$. Positive and negative values of $\tilde{n}_{\mathrm{exc}}(\boldsymbol{q},\boldsymbol{q}';t)$ indicate the existence or absence of the exciton, respectively. If $\tilde{n}_{\mathrm{exc}}(\boldsymbol{q},\boldsymbol{q}';t)$ has a positive value within a very short time scale, such an exciton can be deemed a *transient* exciton.

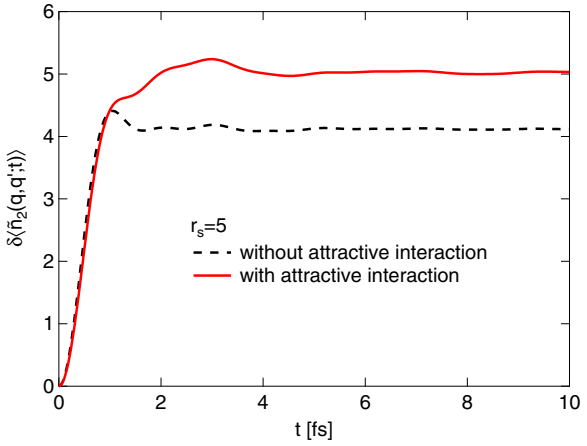

FIG. 2. (Color online) t dependence of $\delta\langle n_2(\boldsymbol{q},\boldsymbol{q}';t)\rangle$ and $\delta\langle n_2^{(0)}(\boldsymbol{q},\boldsymbol{q}';t)\rangle$ (see the text for the definition) for $r_s = 5$. The parameters are $|\boldsymbol{q}| = |\boldsymbol{q}'| = k_F/2$ and $|\boldsymbol{q}+\boldsymbol{q}'| = k_F$.

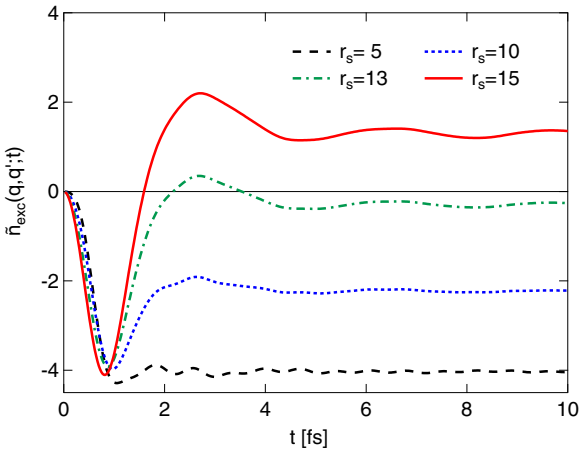

FIG. 3. (Color online) t dependence of $\tilde{n}_{\rm exc}(\boldsymbol{q},\boldsymbol{q}';t)$ for various r_s. The parameters are $|\boldsymbol{q}| = |\boldsymbol{q}'| = k_F/2$ and $|\boldsymbol{q}+\boldsymbol{q}'| = k_F$. Positive values indicate the existence of the exciton.

IV. APPLICATION TO A JELLIUM MODEL

One of the main results in this study is a derivation for the exciton density, as shown in Eqs. (23)–(25). As a trivial example, the application to the exciton in a jellium model without the screening effect is shown because the lifetime of such an exciton is infinite (see Sec. IV A). In Sec. IV B, the transient nature of the exciton is revealed by considering the screening effect. In Sec. IV C, the effect of the higher-order perturbation expansion terms is discussed.

A. Without screening effect

Figure 2 shows t dependence of $\delta\langle n_2(\boldsymbol{q},\boldsymbol{q}';t)\rangle = \sum_{\sigma,\sigma'}\delta\langle n_2(q,q';t)\rangle$ and $\delta\langle n_2^{(0)}(\boldsymbol{q},\boldsymbol{q}';t)\rangle = \sum_{\sigma,\sigma'}\delta\langle n_2^{(0)}(q,q';t)\rangle$, where the former is the EH pair density with the attractive interaction only while the latter is the EH pair density without both the EH attractive interaction and the screening effect. By definition, the difference between them is the exciton density [see Eq. (24)]. The density parameter is set to $r_s = 5$. The exciton density gradually increases after 1 fs and reaches a positive constant at $t \to \infty$. Similar behavior is observed for all r_s. These results show the validity of the definition for the exciton density given in Eqs. (23)–(25).

B. With screening effect

The fundamental properties of the transient exciton are investigated by changing the density parameter r_s and the total momentums $|\boldsymbol{q}+\boldsymbol{q}'|$, in Secs. IVB1 and IVB2, respectively, and the real-space analysis is performed in Sec. IVB3. Finally, in Sec. IVB4, the existence of the transient exciton in the jellium model is discussed.

1. r_s dependence

Figure 3 shows the exciton density in a jellium model calculated using Eq. (23) for $r_s = 5, 10, 13$, and 15. We set $|\boldsymbol{q}| = |\boldsymbol{q}'| = |\boldsymbol{q}+\boldsymbol{q}'|/2 = k_F/2$, i.e., the total momentum of the exciton is k_F, while the relative momentum is zero. The screening effect in $\tilde{D}_1^{\rm R}(\boldsymbol{q};\omega')$ is treated within the random-phase approximation [12], together with the local-field correction (LFC). The analytic expression for the dielectric screening function given in Ref. [15] is used for the LFC [16]. We compute the integral involving $\tilde{D}_2^{\rm R}(q,q',\sigma'';\omega')$ using the standard Monte Carlo approach. When t is less than 1 fs, $\tilde{n}_{\rm exc}(\boldsymbol{q},\boldsymbol{q}';t)$ decreases for all r_s. When t is larger than 1 fs, $\tilde{n}_{\rm exc}(\boldsymbol{q},\boldsymbol{q}';t)$ begins to increase for large r_s. In the case of $r_s = 13$, $\tilde{n}_{\rm exc}(\boldsymbol{q},\boldsymbol{q}';t)$ is positive only when $t = 2$–4 fs, which can be interpreted as indicating a transient exciton. In the case of $r_s = 15$, on the other hand, $\tilde{n}_{\rm exc}(\boldsymbol{q},\boldsymbol{q}';t)$ is positive when $t > 1.8$ fs, which is interpreted as evidence of a stable exciton [17]. This clearly shows a crossover from a transient to a stable exciton, which is due to the weak screening effect that occurs in low-density electron gas systems.

2. q dependence

Figure 4 shows the t dependence of $\tilde{n}_{\rm exc}(\boldsymbol{q},\boldsymbol{q}';t)$ in the case of $r_s = 7$ for various $|\boldsymbol{q}+\boldsymbol{q}'|$. In the initial stage ($t \sim 10$ fs), large $|\boldsymbol{q}+\boldsymbol{q}'|/k_F = 0.5$–0.7 contributes to exciton formation while, in the final stage ($t > 20$ fs), small $|\boldsymbol{q}+\boldsymbol{q}'|/k_F = 0.3$–0.5 also contributes to the formation. This leads to an increase with time in both the average radius and the spatial period of

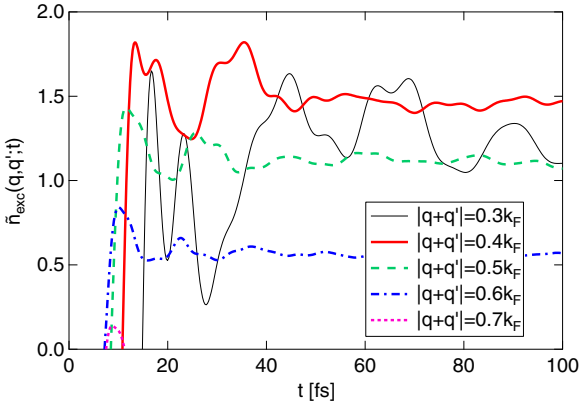

FIG. 4. (Color online) t dependence of $\tilde{n}_{\rm exc}(\boldsymbol{q},\boldsymbol{q}';t)$ for various $|\boldsymbol{q}+\boldsymbol{q}'|$. The density parameter is set to $r_s = 7$.

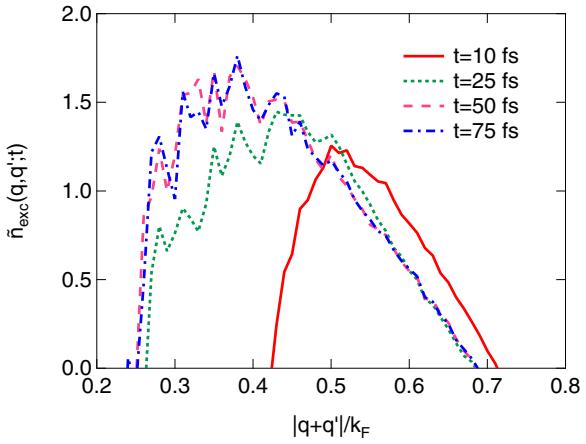

FIG. 5. (Color online) $|\boldsymbol{q}+\boldsymbol{q}'|$ dependence of $\tilde{n}_{\rm exc}(\boldsymbol{q},\boldsymbol{q}';t)$ for $t = 10,25,50$, and 75 fs.

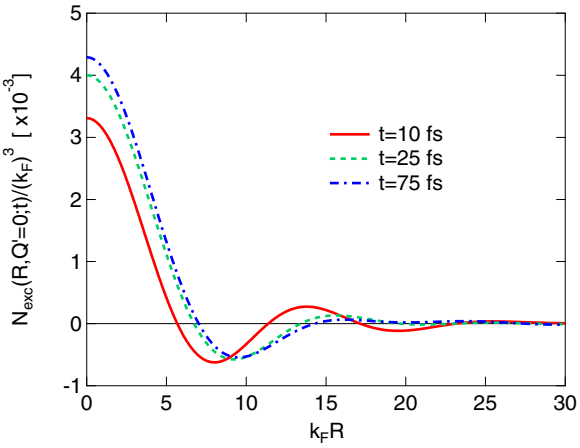

FIG. 6. (Color online) Real-space distribution of $\tilde{N}_{\rm exc}(R;\boldsymbol{Q}'=\boldsymbol{0};t)$ for $t = 10,25$, and 75 fs. The spatial period of the exciton density oscillation increases with time.

the exciton density oscillation in real space, which is a novel property involving the exciton formation. The Fourier analysis of the density in space is given below.

3. Real-space analysis

Figure 5 shows a snapshot of $|\boldsymbol{q}+\boldsymbol{q}'|$ dependence of $\tilde{n}_{\rm exc}(\boldsymbol{q},\boldsymbol{q}';t)$ at $t = 10,25,50$, and 75 fs. At $t = 10$ fs, $\tilde{n}_{\rm exc}(\boldsymbol{q},\boldsymbol{q}';t)$ is positive when $0.42k_F \leqslant |\boldsymbol{q}+\boldsymbol{q}'| \leqslant 0.71k_F$ and takes the maximum at $|\boldsymbol{q}+\boldsymbol{q}'| \simeq 0.5k_F$. As t increases, the value of $\tilde{n}_{\rm exc}(\boldsymbol{q},\boldsymbol{q}';t)$ having small $|\boldsymbol{q}+\boldsymbol{q}'|$ increases: for example, at $t = 75$ fs, the peak of $\tilde{n}_{\rm exc}(\boldsymbol{q},\boldsymbol{q}';t)$ redshifts and the width of $\tilde{n}_{\rm exc}(\boldsymbol{q},\boldsymbol{q}';t)$ increases ($0.25k_F \leqslant |\boldsymbol{q}+\boldsymbol{q}'| \leqslant 0.69k_F$). To study a real-space distribution of excitons, we use the Fourier transformation given by

$$n_{\rm exc}(\boldsymbol{x},\boldsymbol{x}';t) = \int \frac{d\boldsymbol{q}}{(2\pi)^3}\int \frac{d\boldsymbol{q}'}{(2\pi)^3} \times e^{i\boldsymbol{q}\cdot(\boldsymbol{x}-\boldsymbol{x}'')}e^{i\boldsymbol{q}'\cdot(\boldsymbol{x}'-\boldsymbol{x}'')}\tilde{n}_{\rm exc}(\boldsymbol{q},\boldsymbol{q}';t). \tag{26}$$

Let $\boldsymbol{Q}$ and $\boldsymbol{Q}'$ be the total momentum and relative momentum of an exciton, respectively, i.e.,

$$\boldsymbol{Q} = \boldsymbol{q}+\boldsymbol{q}', \quad \boldsymbol{Q}' = \frac{\boldsymbol{q}-\boldsymbol{q}'}{2}. \tag{27}$$

Then, the exciton density can be represented by

$$\begin{aligned} &n_{\rm exc}(\boldsymbol{x},\boldsymbol{x}';t) \\ &= \int \frac{d\boldsymbol{Q}'}{(2\pi)^3}e^{i\boldsymbol{Q}'\cdot(\boldsymbol{x}-\boldsymbol{x}')} \\ &\quad\times\left[\int \frac{d\boldsymbol{Q}}{(2\pi)^3}e^{i\boldsymbol{Q}\cdot\boldsymbol{R}}\tilde{n}_{\rm exc}\left(\frac{\boldsymbol{Q}}{2}+\boldsymbol{Q}',\frac{\boldsymbol{Q}}{2}-\boldsymbol{Q}';t\right)\right] \\ &\equiv \int \frac{d\boldsymbol{Q}'}{(2\pi)^3}e^{i\boldsymbol{Q}'\cdot(\boldsymbol{x}-\boldsymbol{x}')}\tilde{N}_{\rm exc}(\boldsymbol{R};\boldsymbol{Q}';t), \end{aligned} \tag{28}$$

where $\boldsymbol{R} = (\boldsymbol{x}+\boldsymbol{x}'-2\boldsymbol{x}'')/2$ is the position of the center of mass and $\tilde{N}_{\rm exc}(\boldsymbol{R};\boldsymbol{Q}';t)$ is the exciton density in mixed coordinates $\boldsymbol{R}$ and $\boldsymbol{Q}'$. In this work, we study $\tilde{N}_{\rm exc}(\boldsymbol{R};\boldsymbol{Q}'=\boldsymbol{0};t)$ only. The case of $\boldsymbol{Q}' \neq \boldsymbol{0}$ will be studied elsewhere [18]. In a jellium model, the exciton density depends on $R = |\boldsymbol{R}|$ and is written as

$$\begin{aligned} \tilde{N}_{\rm exc}(R;\boldsymbol{Q}'=\boldsymbol{0};t) &= \int \frac{d\boldsymbol{Q}}{(2\pi)^3}e^{i\boldsymbol{Q}\cdot\boldsymbol{R}}\tilde{n}_{\rm exc}\left(\frac{\boldsymbol{Q}}{2},\frac{\boldsymbol{Q}}{2};t\right) \\ &= \frac{1}{2\pi^2 R}\int_0^\infty dQ\,Q\sin(QR)\tilde{n}_{\rm exc}(Q;t). \end{aligned} \tag{29}$$

Figure 6 shows the distribution of $\tilde{N}_{\rm exc}(R;\boldsymbol{Q}'=\boldsymbol{0};t)$ given by Eq. (29) for $t = 10,25$, and 75 fs. At $t = 10$ fs, the exciton exists at the region $k_F R \leqslant 5.6$, $11.4 \leqslant k_F R \leqslant 17.1$, and $23.1 \leqslant k_F R \leqslant 30$, although the magnitude of $\tilde{N}_{\rm exc}(R;\boldsymbol{Q}'=\boldsymbol{0};t)$ decreases drastically as $k_F R$ increases. As t increases, the magnitude of $\tilde{N}_{\rm exc}(R;\boldsymbol{Q}'=\boldsymbol{0};t)$ near $R \simeq 0$ increases and the exciton exists at the region $k_F R \leqslant 7$ and $14.3 \leqslant k_F R \leqslant 27.5$. This means that both the average radius of the exciton and the spatial period of the density oscillation in $\tilde{N}_{\rm exc}(R;\boldsymbol{Q}'=\boldsymbol{0};t)$ increase with time. This is due to an increase in the value of $\tilde{n}_{\rm exc}(\boldsymbol{q},\boldsymbol{q}';t)$ with small $|\boldsymbol{q}+\boldsymbol{q}'|$, as shown in Fig. 5. We expect that the character of the exciton time evolution in a realistic material is qualitatively the same as that in a jellium model.

4. Transient exciton regime

As shown in Fig. 4 (for the case of $r_s = 7$), the stable exciton exists even at $t \to \infty$: the exciton with $|\boldsymbol{q}+\boldsymbol{q}'| = 0.7k_F$ is the transient exciton, whereas those with $|\boldsymbol{q}+\boldsymbol{q}'| = 0.3k_F$ to $0.6k_F$ are the stable exciton. By considering the parameter range $|\boldsymbol{q}+\boldsymbol{q}'| = 0.1k_F$–$1.0k_F$, the specific r_s in which the transient exciton exists only has been investigated. Figure 7 shows t dependence of $\tilde{n}_{\rm exc}(\boldsymbol{q},\boldsymbol{q}';t)$ for $|\boldsymbol{q}+\boldsymbol{q}'|/k_F = 0.3,0.35$, and 0.4. The density parameter was set to $r_s = 4.5$. The transient exciton is clearly observed (positive $\tilde{n}_{\rm exc}$ only when $t = 5$–25 fs), i.e., the exciton density vanishes at $t \to \infty$. On the other hand, no exciton modes were observed for other $|\boldsymbol{q}+\boldsymbol{q}'|$s because $\tilde{n}_{\rm exc}$ with such $|\boldsymbol{q}+\boldsymbol{q}'|$s is negative. Thus, for the specific density $r_s = 4.5$, the sudden creation of a positive charge into a jellium model creates the transient exciton only. Through the thorough investigation, with the density parameter r_s below 4.0 and above 5.0, no exciton modes or stable exciton modes were observed, respectively.

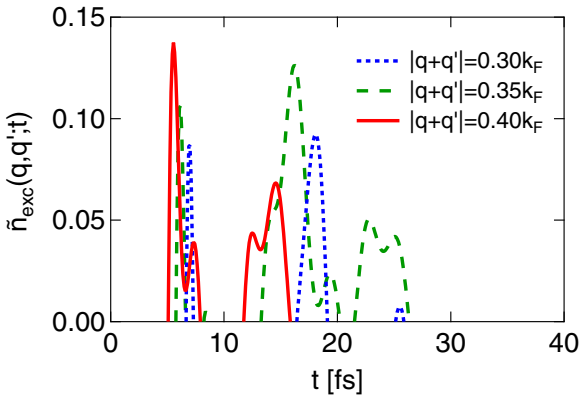

FIG. 7. (Color online) t dependence of $\tilde{n}_{\rm exc}(\boldsymbol{q},\boldsymbol{q}';t)$ for various $|\boldsymbol{q}+\boldsymbol{q}'|$. The density parameter is set to $r_s = 4.5$.

This is physically reasonable because in such a system having a high or low electron density the screening becomes complete or incomplete enough to generate no excitons or stable excitons, respectively. This is also reasonable because most real metals have $r_s = 2$–5.

The transient exciton has been observed at the silver surface by Cui *et al.* [4]. The present calculation suggests that the transient exciton can exist in a small range around $r_s = 4.5$. Based on this result, it could be predicted that the stable exciton should be observed if the electron density is decreased at the silver surface. The chemical adsorption at the surface (such as oxygen adsorption) may be useful to examine the crossover from the transient to stable exciton.

It should be noted that on the femtosecond time scale the existence of the transient exciton is limited by the uncertainty relation between time and energy, i.e., $\Delta t \Delta E \geqslant \hbar/2$: for example, when $\Delta t \sim 1$ fs, we obtain $\Delta E \sim 0.33$ eV. With such a large uncertainty, determining the energy of the transient exciton would be meaningless.

C. Higher-order perturbation expansion

In the $D_2^{\rm T}(x,x',x'';t-t')$ computation, one may find $(2m+3)!$ possible diagrams in the mth order (m is a nonnegative integer) by applying Wick's theorem [12]. The present calculation considers up to the first-order contribution of $D_2^{\rm T}(x,x',x'';t-t')$ [shown in Figs. 1(c) and 1(d)], which are the most fundamental components as regards examination of exciton creation. Note that the inclusion of higher-order terms (such as Fig. 8) may enhance the magnitude of $\tilde{n}_{\rm exc}(\boldsymbol{q},\boldsymbol{q}';t)$. The inclusion of infinite terms leads to nonperturbative treatment, which is desirable for the complete description of the exciton. However, it is quite difficult to perform such a calculation at the present formulation. A new approach for the nonperturbative treatment has to be developed.

V. SUMMARY

The purpose of this paper was to develop a theory to describe the dynamics of excitons with time evolutions that cannot be studied using the effective-mass equation and the standard BSE with stationary interaction potential. The linear response of the EH pair density to an external perturbation was examined. By considering the electron-hole attractive interaction and the screening effect, a definition of exciton density in a first-principles context was derived. Further, the application of the proposed theory to a jellium model confirmed the existence of transient excitons and unveiled the mechanism of exciton formation. Investigating the associated band structure, spin, phonon, and quantum size effects will provide an enhanced understanding of the dynamics of excitons in condensed-matter systems.

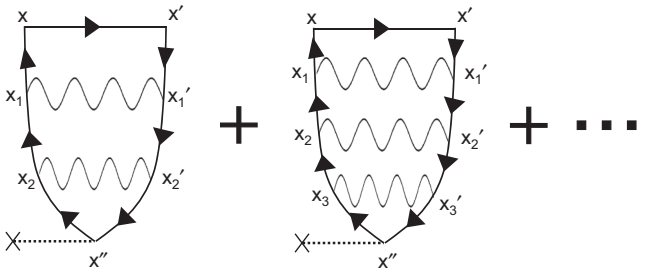

FIG. 8. The second- and third-order contribution to $D_2^{\rm T}(x,x',x'';t-t')$.

ACKNOWLEDGMENTS

The author acknowledges S. G. Louie, M. Bernadi, J. Mustafa, and K. Ohno for their contributions to fruitful discussions. This research was supported by the Computational Materials Research Initiative [High Performance Computing Infrastructure (HPCI), Ministry of Education, Culture, Sports, Science, and Technology (MEXT)] program for Young Researcher Overseas Visits and a grant-in-aid for Scientific Research in Innovative Areas (Grant No. 25104713) from MEXT.

APPENDIX A: ZEROTH-ORDER CONTRIBUTION

First, we calculate the zeroth-order contributions in $\tilde{D}_2^{\rm T}(q,q',\sigma'';\omega)$ via the Fourier transformations. By using the interaction picture $[\psi_I(x;t) = e^{iH_0 t/\hbar}\psi(x)e^{-iH_0 t/\hbar}]$ (the subscript I is omitted for simplicity) and Wick's theorem, the time-ordered product

$$\langle N,0|{\rm T}[\psi^\dagger(x';t)\psi(x;t)\psi^\dagger(x;t)\psi(x';t)\psi^\dagger(x'';t')\psi(x'';t')] \times |N,0\rangle \tag{A1}$$

can be decomposed into six terms:

$$\begin{aligned}
&+ [\psi^\dagger(x';t)\psi(x;t)]_c[\psi^\dagger(x;t)\psi(x';t)]_c[\psi^\dagger(x'';t')\psi(x'';t')]_c,\\
&- [\psi^\dagger(x';t)\psi(x;t)]_c[\psi^\dagger(x;t)\psi(x'';t')]_c[\psi^\dagger(x'';t')\psi(x';t)]_c,\\
&- [\psi^\dagger(x';t)\psi(x';t)]_c[\psi^\dagger(x;t)\psi(x;t)]_c[\psi^\dagger(x'';t')\psi(x'';t')]_c,\\
&+ [\psi^\dagger(x';t)\psi(x';t)]_c[\psi^\dagger(x;t)\psi(x'';t')]_c[\psi^\dagger(x'';t')\psi(x;t)]_c,\\
&+ [\psi^\dagger(x';t)\psi(x'';t')]_c[\psi^\dagger(x;t)\psi(x;t)]_c[\psi^\dagger(x'';t')\psi(x';t)]_c,\\
&- [\psi^\dagger(x';t)\psi(x'';t')]_c[\psi^\dagger(x;t)\psi(x';t)]_c[\psi^\dagger(x'';t')\psi(x;t)]_c,
\end{aligned} \tag{A2}$$

where $[\cdots]_c$ denotes the contraction (see Ref. [12]), which is expressed by the noninteracting Green's function via the

relations

$$[\psi^\dagger(x';t)\psi(x'';t')]_c = -iG^{(0)}(x'',x';t'-t), \quad \text{(A3)}$$

$$[\psi^\dagger(x;t)\psi(x';t)]_c = -iG^{(0)}(x',x;t-t^+). \quad \text{(A4)}$$

The Fourier transformation in time of Eq. (A2) multiplied by $(-i)$ yields the zeroth-order contributions $D_2^{\mathrm{T}(0)}(x,x',x'';\omega)$. The first and third terms in Eq. (A2) give $\mathrm{Im}D_2^{\mathrm{T}(0)}(x,x',x'';\omega) \propto \delta(\omega)$, which does not contribute $\delta\langle\tilde{n}_2(q,q';t)\rangle$ because $(1-\cos\omega t)/\omega \to 0$ [see Eqs. (21) and (22)]. Thus, the zeroth-order contribution $D_2^{\mathrm{T}(0)}(x,x',x'';\omega)$ is expressed by the sum of four terms:

$$D_2^{\mathrm{T}(0)}(x,x',x'';\omega) = \sum_{i=1}^{4} D_2^{\mathrm{T}(0-i)}(x,x',x'';\omega), \quad \text{(A5)}$$

where

$$D_2^{\mathrm{T}(0-1)}(x,x',x'';\omega) = \delta_{\sigma\sigma'}\delta_{\sigma''\sigma}\delta_{\sigma'\sigma''}(-1)\left(i\sum_{\alpha}^{\mathrm{occ}}\phi_{\alpha\sigma}(\boldsymbol{x})\phi^*_{\alpha\sigma}(\boldsymbol{x}')\right)\int\frac{d\omega'}{2\pi}G^{(0)}_{\sigma''}(\boldsymbol{x}'',\boldsymbol{x};\omega')G^{(0)}_{\sigma'}(\boldsymbol{x}',\boldsymbol{x}'';\omega+\omega'),$$

$$D_2^{\mathrm{T}(0-2)}(x,x',x'';\omega) = \delta_{\sigma'\sigma'}\delta_{\sigma''\sigma}\delta_{\sigma\sigma''}\left(i\sum_{\alpha}^{\mathrm{occ}}|\phi_{\alpha\sigma'}(\boldsymbol{x}')|^2\right)\int\frac{d\omega'}{2\pi}G^{(0)}_{\sigma''}(\boldsymbol{x}'',\boldsymbol{x};\omega')G^{(0)}_{\sigma}(\boldsymbol{x},\boldsymbol{x}'';\omega+\omega'),$$

$$D_2^{\mathrm{T}(0-3)}(x,x',x'';\omega) = \delta_{\sigma\sigma}\delta_{\sigma''\sigma'}\delta_{\sigma'\sigma''}\left(i\sum_{\alpha}^{\mathrm{occ}}|\phi_{\alpha\sigma}(\boldsymbol{x})|^2\right)\int\frac{d\omega'}{2\pi}G^{(0)}_{\sigma''}(\boldsymbol{x}'',\boldsymbol{x}';\omega')G^{(0)}_{\sigma'}(\boldsymbol{x}',\boldsymbol{x}'';\omega+\omega'),$$

$$D_2^{\mathrm{T}(0-4)}(x,x',x'';\omega) = \delta_{\sigma'\sigma}\delta_{\sigma''\sigma'}\delta_{\sigma\sigma''}(-1)\left(i\sum_{\alpha}^{\mathrm{occ}}\phi_{\alpha\sigma'}(\boldsymbol{x}')\phi^*_{\alpha\sigma'}(\boldsymbol{x})\right)\int\frac{d\omega'}{2\pi}G^{(0)}_{\sigma''}(\boldsymbol{x}'',\boldsymbol{x}';\omega')G^{(0)}_{\sigma}(\boldsymbol{x},\boldsymbol{x}'';\omega+\omega').$$

The integration for ω' can be evaluated by using the expression

$$\int\frac{d\omega'}{2\pi}G^{(0)}_{\sigma'}(\boldsymbol{x}',\boldsymbol{x}'';\omega')G^{(0)}_{\sigma}(\boldsymbol{x},\boldsymbol{x}''';\omega+\omega') = i\sum_{c}^{\mathrm{emp}}\sum_{v}^{\mathrm{occ}}\left[\frac{\phi_{c\sigma}(\boldsymbol{x})\phi_{v\sigma'}(\boldsymbol{x}')\phi^*_{v\sigma'}(\boldsymbol{x}'')\phi^*_{c\sigma}(\boldsymbol{x}''')}{\omega-(\omega_{\boldsymbol{k}_c}-\omega_{\boldsymbol{k}_v})+i\delta} - \frac{\phi_{v\sigma}(\boldsymbol{x})\phi_{c\sigma'}(\boldsymbol{x}')\phi^*_{c\sigma'}(\boldsymbol{x}'')\phi^*_{v\sigma}(\boldsymbol{x}''')}{\omega-(\omega_{\boldsymbol{k}_v}-\omega_{\boldsymbol{k}_c})-i\delta}\right], \quad \text{(A6)}$$

the imaginary part of which is calculated by using the identity $(\omega\pm i\delta)^{-1} = \mathcal{P}\omega^{-1} \mp i\pi\delta(\omega)$ valid for real ω. In the following, we calculate these four terms relevant to an increase in the EH pair density.

1. First term

The contribution from $D_2^{\mathrm{T}(0-1)}(x,x',x'';\omega)$ corresponds to the that from Fig. 1(b). By using Eq. (15), $D_2^{\mathrm{T}(0-1)}(x,x',x'';\omega)$ is written as

$$D_2^{\mathrm{T}(0-1)}(x,x',x'';\omega) = \delta_{\sigma\sigma'}\delta_{\sigma''\sigma}\delta_{\sigma'\sigma''}\int\frac{d\boldsymbol{k}_\alpha}{(2\pi)^3}\int\frac{d\boldsymbol{k}_c}{(2\pi)^3}\int\frac{d\boldsymbol{k}_v}{(2\pi)^3}\theta_H(k_F-|\boldsymbol{k}_\alpha|)\theta_H(|\boldsymbol{k}_c|-k_F)\theta_H(k_F-|\boldsymbol{k}_v|)$$
$$\times\left[\frac{e^{i(\boldsymbol{k}_\alpha-\boldsymbol{k}_v)\cdot(\boldsymbol{x}-\boldsymbol{x}'')}e^{i(\boldsymbol{k}_c-\boldsymbol{k}_\alpha)\cdot(\boldsymbol{x}'-\boldsymbol{x}'')}}{\omega-(\omega_{\boldsymbol{k}_c}-\omega_{\boldsymbol{k}_v})+i\delta} - \frac{e^{i(\boldsymbol{k}_\alpha-\boldsymbol{k}_c)\cdot(\boldsymbol{x}-\boldsymbol{x}'')}e^{i(\boldsymbol{k}_v-\boldsymbol{k}_\alpha)\cdot(\boldsymbol{x}'-\boldsymbol{x}'')}}{\omega-(\omega_{\boldsymbol{k}_v}-\omega_{\boldsymbol{k}_c})-i\delta}\right]. \quad \text{(A7)}$$

The Fourier transformation in space of $D_2^{\mathrm{T}(0-1)}(x,x',x'';\omega)$ yields

$$\tilde{D}_2^{\mathrm{T}(0-1)}(q,q',\sigma'';\omega) = \delta_{\sigma\sigma'}\delta_{\sigma''\sigma}\delta_{\sigma'\sigma''}\int\frac{d\boldsymbol{k}_v}{(2\pi)^3}\theta(k_F-|\boldsymbol{k}_v|)$$
$$\times\left[\frac{\theta_H(|\boldsymbol{k}_v+\boldsymbol{q}+\boldsymbol{q}'|-k_F)\theta_H(k_F-|\boldsymbol{k}_v+\boldsymbol{q}|)}{\omega-(\omega_{\boldsymbol{k}_v+\boldsymbol{q}+\boldsymbol{q}'}-\omega_{\boldsymbol{k}_v})+i\delta} - \frac{\theta_H(|\boldsymbol{k}_v-\boldsymbol{q}-\boldsymbol{q}'|-k_F)\theta_H(k_F-|\boldsymbol{k}_v-\boldsymbol{q}'|)}{\omega-(\omega_{\boldsymbol{k}_v}-\omega_{\boldsymbol{k}_v-\boldsymbol{q}-\boldsymbol{q}'})-i\delta}\right], \quad \text{(A8)}$$

the imaginary part of which is given as

$$\mathrm{Im}\tilde{D}_2^{\mathrm{T}(0-1)}(q,q',\sigma'';\omega) = \delta_{\sigma\sigma'}\delta_{\sigma''\sigma}\delta_{\sigma'\sigma''}(-\pi)\int\frac{d\boldsymbol{k}_v}{(2\pi)^3}\theta(k_F-|\boldsymbol{k}_v|)$$
$$\times\big[\theta_H(|\boldsymbol{k}_v+\boldsymbol{q}+\boldsymbol{q}'|-k_F)\theta_H(k_F-|\boldsymbol{k}_v+\boldsymbol{q}|)\delta\big(\omega-\omega_{\boldsymbol{k}_v+\boldsymbol{q}+\boldsymbol{q}'}+\omega_{\boldsymbol{k}_v}\big)$$
$$+\theta_H(|\boldsymbol{k}_v-\boldsymbol{q}-\boldsymbol{q}'|-k_F)\theta_H(k_F-|\boldsymbol{k}_v-\boldsymbol{q}'|)\delta\big(\omega-\omega_{\boldsymbol{k}_v}+\omega_{\boldsymbol{k}_v-\boldsymbol{q}-\boldsymbol{q}'}\big)\big]. \quad \text{(A9)}$$

Since $\omega_{\boldsymbol{k}_c} - \omega_{\boldsymbol{k}_v} > 0$ and $\omega > 0$, the second term in the square bracket of this equation vanishes. Thus, we obtain

$$\mathrm{Im}\tilde{D}_2^{\mathrm{T}(0-1)}(q,q',\sigma'';\omega) = \delta_{\sigma\sigma'}\delta_{\sigma''\sigma}\delta_{\sigma'\sigma''}(-\pi)\int \frac{d\boldsymbol{k}_v}{(2\pi)^3}\theta_H(k_F - |\boldsymbol{k}_v|)\theta_H(|\boldsymbol{k}_v+\boldsymbol{q}+\boldsymbol{q}'| - k_F)\theta_H(k_F - |\boldsymbol{k}_v+\boldsymbol{q}|) \times\delta\left(\omega - \frac{\hbar|\boldsymbol{k}_v+\boldsymbol{q}+\boldsymbol{q}'|^2}{2m} + \frac{\hbar k_v^2}{2m}\right). \tag{A10}$$

$\mathrm{Im}\tilde{D}_2^{\mathrm{T}(0-1)}(q,q',\sigma'';\omega)$ has a negative sign and depends on both the magnitude of vectors, $|\boldsymbol{q}+\boldsymbol{q}'|$ and $|\boldsymbol{q}|$, and the angle θ between $\boldsymbol{q}+\boldsymbol{q}'$ and $\boldsymbol{q}$.

2. Second and third terms

Similarly to the derivation of $\tilde{D}_2^{\mathrm{T}(0-1)}(q,q',\sigma'';\omega)$, we obtain the imaginary part of $\tilde{D}_2^{\mathrm{T}(0-2)}(q,q',\sigma'';\omega)$ for $\omega > 0$:

$$\mathrm{Im}\tilde{D}_2^{\mathrm{T}(0-2)}(q,q',\sigma'';\omega) = \delta_{\sigma'\sigma'}\delta_{\sigma''\sigma}\delta_{\sigma\sigma''}\frac{mk_F^3\delta(\boldsymbol{q}')}{6\pi\hbar}\int d\boldsymbol{k}\theta_H(|\boldsymbol{k}+\boldsymbol{q}| - k_F)\theta_H(k_F - |\boldsymbol{k}|)\delta\left(\boldsymbol{k}\cdot\boldsymbol{q} + \frac{|\boldsymbol{q}|^2}{2} - \frac{m\omega}{\hbar}\right). \tag{A11}$$

The calculation of the integral for $\boldsymbol{k}$ is the same as that of the noninteracting polarization function (see Ref. [12]). The third term $\tilde{D}_2^{\mathrm{T}(0-3)}(q,q',\sigma'';\omega)$ is obtained by transforming $\boldsymbol{q} \leftrightarrow \boldsymbol{q}'$ for the expression in $\tilde{D}_2^{\mathrm{T}(0-2)}(q,q',\sigma'';\omega)$. If we assume that the total momentum of the exciton is not zero (i.e., $|\boldsymbol{q}+\boldsymbol{q}'| \neq 0$) and the electron and hole move along the same direction (i.e., $\boldsymbol{q}//\boldsymbol{q}'$), $\boldsymbol{q}$ and $\boldsymbol{q}'$ are not equal to zero. In this assumption, these terms, $\tilde{D}_2^{\mathrm{T}(0-2)}(q,q',\sigma'';\omega)$ and $\tilde{D}_2^{\mathrm{T}(0-3)}(q,q',\sigma'';\omega)$, do not contribute to an increase in the EH pair density due to the presence of the factors $\delta(\boldsymbol{q}')$ and $\delta(\boldsymbol{q})$.

3. Fourth term

The contribution from $D_2^{\mathrm{T}(0-4)}(x,x',x'';\omega)$ corresponds to that from Fig. 1(a). This term can be obtained by transforming $\boldsymbol{q} \leftrightarrow \boldsymbol{q}'$ for the expression in $\tilde{D}_2^{\mathrm{T}(0-1)}(q,q',\sigma'';\omega)$. Thus, the imaginary part of $\tilde{D}_2^{\mathrm{T}(0-4)}(q,q',\sigma'';\omega)$ for $\omega > 0$ is given as

$$\mathrm{Im}\tilde{D}_2^{\mathrm{T}(0-4)}(q,q',\sigma'';\omega) = \delta_{\sigma'\sigma}\delta_{\sigma''\sigma'}\delta_{\sigma\sigma''}(-\pi)\int \frac{d\boldsymbol{k}_v}{(2\pi)^3}\theta_H(k_F - |\boldsymbol{k}_v|)\theta_H(|\boldsymbol{k}_v+\boldsymbol{q}+\boldsymbol{q}'| - k_F)\theta_H(k_F - |\boldsymbol{k}_v+\boldsymbol{q}'|) \times\delta\left(\omega - \frac{\hbar|\boldsymbol{k}_v+\boldsymbol{q}+\boldsymbol{q}'|^2}{2m} + \frac{\hbar k_v^2}{2m}\right). \tag{A12}$$

$\mathrm{Im}\tilde{D}_2^{\mathrm{T}(0-4)}(q,q',\sigma'';\omega)$ has a negative sign and depends on both the magnitude of vectors, $|\boldsymbol{q}+\boldsymbol{q}'|$ and $|\boldsymbol{q}'|$, and the angle θ between $\boldsymbol{q}+\boldsymbol{q}'$ and $\boldsymbol{q}'$.

4. Formulas for the integral for the zeroth-order terms

The integral that appeared in $\mathrm{Im}\tilde{D}_2^{\mathrm{T}(0-1)}(q,q',\sigma'';\omega)$ and $\mathrm{Im}\tilde{D}_2^{\mathrm{T}(0-4)}(q,q',\sigma'';\omega)$ can be calculated analytically. Now we focus on the computation of $\mathrm{Im}\tilde{D}_2^{\mathrm{T}(0-4)}(q,q',\sigma'';\omega)$. The result for $\mathrm{Im}\tilde{D}_2^{\mathrm{T}(0-1)}(q,q',\sigma'';\omega)$ will be obtained by replacing $\boldsymbol{q} \leftrightarrow \boldsymbol{q}'$ in the result for $\mathrm{Im}\tilde{D}_2^{\mathrm{T}(0-4)}(q,q',\sigma'';\omega)$ shown below.

The method for calculating the noninteracting polarization function (see Ref. [12]) is useful for performing the integral of $\boldsymbol{k}_v$ in Eq. (A12). The δ function in Eq. (A12) is modified into

$$\delta\left(\omega - \frac{\hbar|\boldsymbol{k}_v+\boldsymbol{q}+\boldsymbol{q}'|^2}{2m} + \frac{\hbar k_v^2}{2m}\right) = \frac{m}{\hbar}\delta\left[\boldsymbol{k}_v\cdot(\boldsymbol{q}+\boldsymbol{q}') + \frac{|\boldsymbol{q}+\boldsymbol{q}'|^2}{2} - \frac{m\omega}{\hbar}\right]. \tag{A13}$$

Since the vector $\boldsymbol{k}_v$ satisfying the equation

$$\boldsymbol{k}_v\cdot(\boldsymbol{q}+\boldsymbol{q}') + \frac{|\boldsymbol{q}+\boldsymbol{q}'|^2}{2} - \frac{m\omega}{\hbar} = (\boldsymbol{k}_v - \boldsymbol{k}_0)\cdot(\boldsymbol{q}+\boldsymbol{q}') = 0 \tag{A14}$$

represents the plane perpendicular to the vector $(\boldsymbol{q}+\boldsymbol{q}')$, the integral for $\boldsymbol{k}_v$ represents the area of the intersection of a part of the Fermi sphere with the plane $(\boldsymbol{k}_v - \boldsymbol{k}_0)\cdot(\boldsymbol{q}+\boldsymbol{q}') = 0$, where $\boldsymbol{k}_0$ is given by

$$\boldsymbol{k}_0 = z_0\frac{\boldsymbol{q}+\boldsymbol{q}'}{|\boldsymbol{q}+\boldsymbol{q}'|},\ z_0 = \frac{m\omega}{\hbar|\boldsymbol{q}+\boldsymbol{q}'|} - \frac{|\boldsymbol{q}+\boldsymbol{q}'|}{2}. \tag{A15}$$

The part of the Fermi sphere that contributes the integral is determined by the Heaviside step functions θ_H in Eq. (A12). To perform the integral for $\boldsymbol{k}_v$, we first consider three spheres:

$$S_0 : x^2 + y^2 + z^2 = k_F^2,$$
$$S_1 : (x + |\boldsymbol{q}'|\sin\theta)^2 + y^2 + (z + |\boldsymbol{q}'|\cos\theta)^2 = k_F^2,$$
$$S_2 : x^2 + y^2 + (z + |\boldsymbol{q}+\boldsymbol{q}'|)^2 = k_F^2.$$

Next, we define the circles C_0, C_1, and C_2 as the intersection of the plane $z = z_0$ with the sphere S_0, S_1, and S_2, respectively:

$$C_0 : x^2 + y^2 = r_0^2,$$
$$C_1 : (x + |\boldsymbol{q}'| \sin\theta)^2 + y^2 = r_1^2,$$
$$C_2 : x^2 + y^2 = r_2^2,$$

where

$$r_0 = \sqrt{k_F^2 - z_0^2},$$
$$r_1 = \sqrt{k_F^2 - (z_0 + |\boldsymbol{q}'| \cos\theta)^2},$$
$$r_2 = \sqrt{k_F^2 - (z_0 + |\boldsymbol{q} + \boldsymbol{q}'|)^2}.$$

If we define I_{ij} as the area of the intersection of the sphere S_i with S_j, we obtain

$$I_{00} = \pi\left(k_F^2 - z_0^2\right),$$
$$I_{11} = \pi\left[k_F^2 - (z_0 + |\boldsymbol{q}'| \cos\theta)^2\right],$$
$$I_{22} = \pi\left[k_F^2 - (z_0 + |\boldsymbol{q} + \boldsymbol{q}'|)^2)\right],$$
$$I_{01} = 2(I_{01}^- + I_{01}^+),$$
$$I_{12} = 2(I_{12}^- + I_{12}^+),$$

where

$$I_{01}^- = \int_{x_{01}^-}^{x_{01}} \sqrt{\left(k_F^2 - z_0^2\right) - x^2}\, dx,$$

$$I_{01}^+ = \int_{x_{01}}^{x_{01}^+} \sqrt{k_F^2 - (z_0 + |\boldsymbol{q}'| \cos\theta)^2 - (x + |\boldsymbol{q}'| \sin\theta)^2}\, dx,$$

$$x_{01}^- = -\sqrt{k_F^2 - z_0^2},$$

$$x_{01}^+ = -|\boldsymbol{q}'| \sin\theta + \sqrt{k_F^2 - (z_0 + |\boldsymbol{q}'| \cos\theta)^2},$$

$$x_{01} = -\frac{|\boldsymbol{q}'| + 2z_0 \cos\theta}{2 \sin\theta},$$

and

$$I_{12}^- = \int_{x_{12}^-}^{x_{12}} \sqrt{k_F^2 - (z_0 + |\boldsymbol{q} + \boldsymbol{q}'|)^2 - x^2}\, dx,$$

$$I_{12}^+ = \int_{x_{12}}^{x_{12}^+} \sqrt{k_F^2 - (z_0 + |\boldsymbol{q}'| \cos\theta)^2 - (x + |\boldsymbol{q}'| \sin\theta)^2}\, dx,$$

$$x_{12}^- = -\sqrt{k_F^2 - (z_0 + |\boldsymbol{q} + \boldsymbol{q}'|)^2},$$

$$x_{12}^+ = -|\boldsymbol{q}'| \sin\theta + \sqrt{k_F^2 - (z_0 + |\boldsymbol{q}'| \cos\theta)^2},$$

$$x_{12} = \frac{|\boldsymbol{q} + \boldsymbol{q}'|^2 + 2z_0|\boldsymbol{q} + \boldsymbol{q}'| - 2|\boldsymbol{q}'|z_0 \cos\theta - |\boldsymbol{q}'|^2}{2|\boldsymbol{q}'| \sin\theta}.$$

Here x_{01} and x_{12} are the solutions of simultaneous equations C_0 and C_1 and equations C_1 and C_2, respectively. The definite integrals of $I_{01}^{\pm}$ and $I_{12}^{\pm}$ are calculated analytically. By using these expressions, the value of $\mathrm{Im}\tilde{D}_2^{\mathrm{T}(0-4)}(q,q',\sigma'';\omega)$ is expressed by

$$\mathrm{Im}\tilde{D}_2^{\mathrm{T}(0-4)}(q,q',\sigma'';\omega) = \delta_{\sigma'\sigma}\delta_{\sigma''\sigma'}\delta_{\sigma\sigma''}\left[-\frac{m\pi}{(2\pi)^3\hbar|\boldsymbol{q} + \boldsymbol{q}'|}\right] \times \sum_{ij} \alpha_{ij} I_{ij}, \tag{A16}$$

where $\alpha_{ij} = -1,0,1$, the value of which is determined by $|\boldsymbol{q} + \boldsymbol{q}'|$, $|\boldsymbol{q}'|$, and θ.

APPENDIX B: FIRST-ORDER CONTRIBUTION

In this section, we treat the electron-electron interaction Hamiltonian H_1 in Eq. (8) as a perturbation and derive the first-order contribution to $D_2^{\mathrm{T}}(x,x',x'';t-t')$ shown in Figs. 1(c) and 1(d). The contribution from Fig. 1(c) is given by

$$(-1)(-i)\left(-\frac{i}{\hbar}\right)\frac{1}{2}\int dx_1 \int dx_1' \int dt_1 \int dt_1' V(\boldsymbol{x}_1 - \boldsymbol{x}_1')\delta(t_1 - t_1') \times [-iG^{(0)}(x_1,x'';t_1 - t')][-iG^{(0)}(x,x_1;t - t_1)][-iG^{(0)}(x',x;t - t^+)] \times [-iG^{(0)}(x_1',x';t_1' - t)][-iG^{(0)}(x'',x_1';t' - t_1')], \tag{B1}$$

where (-1) denotes a closed loop and $(-i)$ comes from the definition of the time-ordered correlation function. The Fourier transformation in time of Eq. (B1) yields

$$(-1)(-i)^6\left(-\frac{i}{\hbar}\right)\frac{1}{2}\int dx_1 \int dx_1' V(\boldsymbol{x}_1 - \boldsymbol{x}_1')\delta_{\sigma_1\sigma''}\delta_{\sigma\sigma_1}\delta_{\sigma'\sigma}\delta_{\sigma_1'\sigma'}\delta_{\sigma''\sigma_1'}\left(i\sum_{\alpha}^{\mathrm{occ}} \phi_{\alpha\sigma'}(\boldsymbol{x}')\phi_{\alpha\sigma'}^*(\boldsymbol{x})\right) \times \int \frac{d\omega_1}{2\pi} \int \frac{d\omega_2}{2\pi} G^{(0)}(\boldsymbol{x}_1,\boldsymbol{x}'';\omega_1)G^{(0)}(\boldsymbol{x},\boldsymbol{x}_1;\omega_2)G^{(0)}(\boldsymbol{x}_1',\boldsymbol{x}';\omega_2 - \omega)G^{(0)}(\boldsymbol{x}'',\boldsymbol{x}_1';\omega_1 - \omega). \tag{B2}$$

The Fourier transformation in space of Eq. (B2) yields

$$\delta_{\sigma''\sigma}\delta_{\sigma'\sigma}\delta_{\sigma'\sigma''}\left(-\frac{1}{2\hbar}\right)\int \frac{d\boldsymbol{k}_\alpha d\boldsymbol{k}_v}{(2\pi)^6}\theta(|\boldsymbol{k}_v + \boldsymbol{q} + \boldsymbol{q}'| - k_F)\theta(k_F - |\boldsymbol{k}_v|)\theta(k_F - |\boldsymbol{k}_\alpha|)\tilde{V}(\boldsymbol{k}_\alpha - \boldsymbol{k}_v - \boldsymbol{q}') \times\left[\frac{\theta(k_F - |\boldsymbol{k}_\alpha - \boldsymbol{q}'|)\theta(|\boldsymbol{k}_\alpha + \boldsymbol{q}| - k_F)}{\left(\omega - \omega_{\boldsymbol{k}_v+\boldsymbol{q}+\boldsymbol{q}'} + \omega_{\boldsymbol{k}_v} + i\delta\right)\left(\omega - \omega_{\boldsymbol{k}_\alpha+\boldsymbol{q}} + \omega_{\boldsymbol{k}_\alpha-\boldsymbol{q}'} + i\delta\right)} - \frac{\theta(k_F - |\boldsymbol{k}_\alpha + \boldsymbol{q}|)\theta(|\boldsymbol{k}_\alpha - \boldsymbol{q}'| - k_F)}{\left(\omega - \omega_{\boldsymbol{k}_v+\boldsymbol{q}+\boldsymbol{q}'} + \omega_{\boldsymbol{k}_v} + i\delta\right)\left(\omega - \omega_{\boldsymbol{k}_\alpha+\boldsymbol{q}} + \omega_{\boldsymbol{k}_\alpha-\boldsymbol{q}'} - i\delta\right)}\right]$$

$$+\delta_{\sigma''\sigma}\delta_{\sigma'\sigma}\delta_{\sigma'\sigma''}\left(-\frac{1}{2\hbar}\right)\int\frac{d\boldsymbol{k}_\alpha d\boldsymbol{k}_v}{(2\pi)^6}\theta(|\boldsymbol{k}_v-\boldsymbol{q}-\boldsymbol{q}'|-k_F)\theta(k_F-|\boldsymbol{k}_v|)\theta(k_F-|\boldsymbol{k}_\alpha|)\tilde{V}(\boldsymbol{k}_\alpha-\boldsymbol{k}_v+\boldsymbol{q})$$
$$\times\left[-\frac{\theta(k_F-|\boldsymbol{k}_\alpha-\boldsymbol{q}'|)\theta(|\boldsymbol{k}_\alpha+\boldsymbol{q}|-k_F)}{\left(\omega-\omega_{\boldsymbol{k}_v}+\omega_{\boldsymbol{k}_v-\boldsymbol{q}-\boldsymbol{q}'}-i\delta\right)\left(\omega-\omega_{\boldsymbol{k}_\alpha+\boldsymbol{q}}+\omega_{\boldsymbol{k}_\alpha-\boldsymbol{q}'}+i\delta\right)}+\frac{\theta(k_F-|\boldsymbol{k}_\alpha+\boldsymbol{q}|)\theta(|\boldsymbol{k}_\alpha-\boldsymbol{q}'|-k_F)}{\left(\omega-\omega_{\boldsymbol{k}_v}+\omega_{\boldsymbol{k}_v-\boldsymbol{q}-\boldsymbol{q}'}-i\delta\right)\left(\omega-\omega_{\boldsymbol{k}_\alpha+\boldsymbol{q}}+\omega_{\boldsymbol{k}_\alpha-\boldsymbol{q}'}-i\delta\right)}\right]. \tag{B3}$$

Since we consider $\omega>0$, the imaginary part of Eq. (B3) is

$$\delta_{\sigma''\sigma}\delta_{\sigma'\sigma}\delta_{\sigma'\sigma''}(I_1+I_2+I_3+I_4), \tag{B4}$$

where

$$I_1=\left(-\frac{1}{2\hbar}\right)\int\frac{d\boldsymbol{k}_\alpha d\boldsymbol{k}_v}{(2\pi)^6}\theta(|\boldsymbol{k}_v+\boldsymbol{q}+\boldsymbol{q}'|-k_F)\theta(k_F-|\boldsymbol{k}_v|)\theta(k_F-|\boldsymbol{k}_\alpha|)\tilde{V}(\boldsymbol{k}_\alpha-\boldsymbol{k}_v-\boldsymbol{q}')$$
$$\times(-\pi)\mathcal{P}\left(\frac{\theta(k_F-|\boldsymbol{k}_\alpha-\boldsymbol{q}'|)\theta(|\boldsymbol{k}_\alpha+\boldsymbol{q}|-k_F)}{\omega-\omega_{\boldsymbol{k}_v+\boldsymbol{q}+\boldsymbol{q}'}+\omega_{\boldsymbol{k}_v}}\right)\delta\left(\omega-\omega_{\boldsymbol{k}_\alpha+\boldsymbol{q}}+\omega_{\boldsymbol{k}_\alpha-\boldsymbol{q}'}\right), \tag{B5}$$

$$I_2=\left(-\frac{1}{2\hbar}\right)\int\frac{d\boldsymbol{k}_\alpha d\boldsymbol{k}_v}{(2\pi)^6}\theta(|\boldsymbol{k}_v+\boldsymbol{q}+\boldsymbol{q}'|-k_F)\theta(k_F-|\boldsymbol{k}_v|)\theta(k_F-|\boldsymbol{k}_\alpha|)\tilde{V}(\boldsymbol{k}_\alpha-\boldsymbol{k}_v-\boldsymbol{q}')$$
$$\times(-\pi)\mathcal{P}\left(\frac{\theta(k_F-|\boldsymbol{k}_\alpha-\boldsymbol{q}'|)\theta(|\boldsymbol{k}_\alpha+\boldsymbol{q}|-k_F)}{\omega-\omega_{\boldsymbol{k}_\alpha+\boldsymbol{q}}+\omega_{\boldsymbol{k}_\alpha-\boldsymbol{q}'}}\right)\delta\left(\omega-\omega_{\boldsymbol{k}_v+\boldsymbol{q}+\boldsymbol{q}'}+\omega_{\boldsymbol{k}_v}\right), \tag{B6}$$

$$I_3=\left(-\frac{1}{2\hbar}\right)\int\frac{d\boldsymbol{k}_\alpha d\boldsymbol{k}_v}{(2\pi)^6}\theta(|\boldsymbol{k}_v+\boldsymbol{q}+\boldsymbol{q}'|-k_F)\theta(k_F-|\boldsymbol{k}_v|)\theta(k_F-|\boldsymbol{k}_\alpha|)\tilde{V}(\boldsymbol{k}_\alpha-\boldsymbol{k}_v-\boldsymbol{q}')$$
$$\times(+\pi)\mathcal{P}\left(\frac{\theta(k_F-|\boldsymbol{k}_\alpha+\boldsymbol{q}|)\theta(|\boldsymbol{k}_\alpha-\boldsymbol{q}'|-k_F)}{\omega-\omega_{\boldsymbol{k}_\alpha+\boldsymbol{q}}+\omega_{\boldsymbol{k}_\alpha-\boldsymbol{q}'}}\right)\delta\left(\omega-\omega_{\boldsymbol{k}_v+\boldsymbol{q}+\boldsymbol{q}'}+\omega_{\boldsymbol{k}_v}\right), \tag{B7}$$

$$I_4=\left(-\frac{1}{2\hbar}\right)\int\frac{d\boldsymbol{k}_\alpha d\boldsymbol{k}_v}{(2\pi)^6}\theta(|\boldsymbol{k}_v-\boldsymbol{q}-\boldsymbol{q}'|-k_F)\theta(k_F-|\boldsymbol{k}_v|)\theta(k_F-|\boldsymbol{k}_\alpha|)\tilde{V}(\boldsymbol{k}_\alpha-\boldsymbol{k}_v+\boldsymbol{q})$$
$$\times(+\pi)\mathcal{P}\left(\frac{\theta(|\boldsymbol{k}_\alpha+\boldsymbol{q}|-k_F)\theta(k_F-|\boldsymbol{k}_\alpha-\boldsymbol{q}'|)}{\omega-\omega_{\boldsymbol{k}_v}+\omega_{\boldsymbol{k}_v-\boldsymbol{q}-\boldsymbol{q}'}}\right)\delta\left(\omega-\omega_{\boldsymbol{k}_\alpha+\boldsymbol{q}}+\omega_{\boldsymbol{k}_\alpha-\boldsymbol{q}'}\right). \tag{B8}$$

The integral for $\boldsymbol{k}_\alpha$ and $\boldsymbol{k}_v$ is computed by using the standard Monte Carlo approach (10^8 sampling points were used.). To obtain the contribution from Fig. 1(d), the replacement $\boldsymbol{q}\leftrightarrow\boldsymbol{q}'$ is needed in these expressions of I_j ($j=1,2,3,4$). Finally, we can calculate $\mathrm{Im}\tilde{D}_2^{\mathrm{R}}(q,q',\sigma'';\omega)$ that appeared in Eqs. (21) and (22).

[1] M. Rohlfing and S. G. Louie, Electron-hole excitations and optical spectra from first principles, Phys. Rev. B **62**, 4927 (2000).

[2] G. Onida, L. Reining, and A. Rubio, Electronic excitations: Density-functional versus many-body Green's-function approaches, Rev. Mod. Phys. **74**, 601 (2002).

[3] R. J. Elliott, Intensity of optical absorption by excitons, Phys. Rev. **108**, 1384 (1957).

[4] X. Cui, C. Wang, A. Argondizzo, S. G. Roe, B. Gumhalter, and H. Petek, Transient excitons at metal surfaces, Nat. Phys. **10**, 505 (2014).

[5] W. D. Schöne, One- and two-particle phenomena in the electronic lifetimes in metals: Quasiparticles and transient excitons, Int. J. Mod. Phys. B **17**, 5655 (2003).

[6] F. J. Rogers, H. C. Graboske, Jr., and D. J. Harwood, Bound eigenstates of the static screened Coulomb potential, Phys. Rev. A **1**, 1577 (1970).

[7] W. D. Schöne and W. Ekardt, Time-dependent screening of a positive charge distribution in metals: Excitons on an ultrashort time scale, Phys. Rev. B **62**, 13464 (2000).

[8] W. D. Schöne and W. Ekardt, Transient excitonic states in noble metals and Al, Phys. Rev. B **65**, 113112 (2002).

[9] B. Gumhalter, P. Lazić, and N. Došlić, Excitonic precursor states in ultrafast pump-probe spectroscopies of surface bands, Phys. Status Solidi B **247**, 1907 (2010).

[10] L. J. Sham and T. M. Rice, Many-particle derivation of the effective-mass equation for the Wannier exciton, Phys. Rev. **144**, 708 (1966).

[11] C. Attaccalite, M. Grüning, and A. Marini, Real-time approach to the optical properties of solids and nanostructures: Time-dependent Bethe-Salpeter equation, Phys. Rev. B **84**, 245110 (2011).

[12] A. L. Fetter and J. D. Walecka, *Quantum Theory of Many-Particle Systems* (Dover, New York, 2003).

[13] G. Strinati, Application of the Green's functions method to the study of the optical properties of semiconductors, Riv. Nuovo Cimento **11**, 1 (1988).

[14] G. S. Canright, Time-dependent screening in the electron gas, Phys. Rev. B **38**, 1647 (1988).

[15] S. Ichimaru and K. Utsumi, Analytic expression for the dielectric screening function of strongly coupled electron liquids at metallic and lower densities, Phys. Rev. B **24**, 7385 (1981).

[16] It was confirmed that the use of the Hubbard-type formula described in Ref. [15] yields the same qualitative results.

[17] The inclusion of other effects such as electron-phonon interactions causes the exciton lifetime to become finite.

[18] The relative momentum is important to study the exciton dispersion. The dispersion relation of four molecular crystals has been investigated recently [19, 20].

[19] P. Cudazzo, M. Gatti, A. Rubio, and F. Sottile, Frenkel versus charge-transfer exciton dispersion in molecular crystals, Phys. Rev. B **88**, 195152 (2013).

[20] P. Cudazzo, F. Sottile, A. Rubio, and M. Gatti, Exciton dispersion in molecular solids, J. Phys.: Condens. Matter **27**, 113204 (2015).